

Field-Enhanced Phenomena of Gold Nanoparticles[†]

Sanghee Nah,^{‡,§} Linjie Li,^{‡,§} and John T. Fourkas^{*,‡,§,||,¶}

Department of Chemistry and Biochemistry, Institute for Physical Science and Technology, Maryland NanoCenter, and Center for Nanophysics and Advanced Materials, University of Maryland, College Park, Maryland 20742

Received: December 15, 2008; Revised Manuscript Received: February 3, 2009

We investigate the connections between two field-enhanced phenomena of gold nanoparticles: multiphoton-absorption-induced luminescence (MAIL) and metal-enhanced multiphoton absorption polymerization (MEMAP). We observe a strong correlation between the nanoparticles and aggregates that have high efficiency for each process. The results of our studies indicate that for this system, MEMAP is driven not by field-enhanced two-photon absorption of the photoinitiator but rather by single-photon excitation of the photoinitiator by the MAIL emission.

I. Introduction

Interest in the field-enhanced phenomena of noble-metal nanostructures has experienced explosive growth in recent years.^{1,2} For instance, surface-enhanced Raman scattering (SERS)^{3–5} has become a powerful analytical technique that is even capable of detecting signals from single molecules.^{6–11} Similarly, surface-enhanced infrared absorption (SEIRA) can lead to increases in the absorption cross section of vibrations of up to 3 orders of magnitude.^{12–16} Field enhancement has also proven to be a powerful means of increasing the signal in coherent anti-Stokes Raman spectroscopy,^{17–20} among other optical techniques.

Despite the wealth of experimental studies on field-enhanced phenomena of noble-metal nanostructures, theory has yet to explain the extreme enhancements of signals that, for instance, make possible the detection of single molecules via SERS. It is clear that aggregates of nanoparticles can provide considerably larger field enhancements than do individual particles, but even the multiparticle structures that have been examined theoretically do not appear capable of generating the enhancements required to explain many of the phenomena that have been observed.^{11,21,22}

An important experimental tool for understanding field enhancement is the correlation of different field-enhanced phenomena with one another and with nanostructure geometry. This type of strategy, for example, led to the realization that aggregates of particles can have considerably larger SERS signals than do single particles.^{11,23,24} Here we apply such an approach to two other phenomena involving field enhancement: multiphoton-absorption-induced luminescence (MAIL) and metal-enhanced multiphoton absorption polymerization (MEMAP).

MAIL from noble-metal surfaces was first reported in 1986.²⁵ Flat metal surfaces were found to be only weakly luminescent. However, significant enhancement of MAIL was observed on roughened surfaces.²⁵ More recently, MAIL has been observed from nanoparticles,^{26–29} nanorods,³⁰ and other nanostructures^{31–35} composed of noble metals. In the case of gold, MAIL has been

observed to be a two-photon process for 800 nm excitation in most studies.^{27,30,34,35} However, some gold nanoparticles have been found to have extremely large MAIL signals, and in this case MAIL is a three-photon process with 800 nm excitation.²⁶ On the other hand, MAIL from silver nanoparticles is a two-photon process with 800 nm excitation.²⁹ We have proposed that the efficient luminescence following three-photon excitation at 800 nm arises from nanoparticles that have shapes that lead to particularly large electric field enhancements.²⁹

In multiphoton absorption polymerization (MAP),^{36–38} the absorption of two or more photons of light is used to excite photoinitiator molecules that drive polymerization in a prepolymer resin. The photons are of too long of a wavelength to be absorbed individually, and so must be absorbed simultaneously. As a result, the absorption probability scales as the light intensity to the power of the number of photons required for excitation. Excitation, and therefore polymerization, can thus be constrained to occur within the focal volume of a tightly focused laser beam. By using an ultrafast laser, which produces short, intense pulses with a low duty cycle, MAP can be accomplished at low average laser power.

Because multiphoton absorption is a nonlinear optical process, its probability can be increased substantially by field enhancement. The idea behind MEMAP is to take advantage of this field enhancement to perform MAP at laser intensities that would normally be below the threshold for causing polymerization. MEMAP has been reported on gold nanostructures created by shadow-sphere lithography,³⁹ in the controlled gaps of nanoscale gold structures,^{34,40} and at a metal-coated AFM tip.⁴¹ MEMAP has also been observed in arrays of gold nanostructures excited with incoherent light.⁴⁰

Here we present the results of studies in which MAIL and MEMAP were performed on the same set of gold nanoparticles on glass substrates. The particles were also imaged with scanning electron microscopy (SEM) to correlate optical properties with structure. We find that both MAIL and MEMAP are most efficient in small clusters of nanoparticles, and that there is a strong correlation between the two phenomena. Wavelength-dependent studies indicate that the dominant mechanism for MEMAP in our systems is not field-enhanced two-photon absorption, but rather that polymerization is driven by the luminescence generated by MAIL.

[†] Part of the “George C. Schatz Festschrift”.

^{*} To whom correspondence should be addressed. E-mail: fourkas@umd.edu.

[‡] Department of Chemistry and Biochemistry.

[§] Institute for Physical Science and Technology.

^{||} Maryland NanoCenter.

[¶] Center for Nanophysics and Advanced Materials.

[#] These authors contributed equally to the work reported in this paper.

II. Experimental Section

Nanoparticle Synthesis. The preparation of gold nanoparticles was carried out through the citrate-reduction method.^{42–44} As an initial step, 0.139 g of HAuCl_4 was dissolved in 250 mL of distilled water. The solution was brought to a boil, and then 20 mL of a 1 wt % sodium citrate solution was added under rapid stirring. To induce further reduction, boiling was continued for about 20 min. The size of the synthesized gold nanoparticles (26 nm) was measured by both UV/visible absorption and transmission electron microscopy.

Gold nanoparticles were coated with silica shells following literature methods.^{45,46} A 500 μL sample of an aqueous solution of 1 mM (3-aminopropyl)trimethoxysilane (APTS) was added slowly to 100 mL of an Au nanoparticle solution under vigorous stirring and allowed to react for 15 min. Next 1 g of sodium silicate solution was diluted to 50 mL with distilled water. The pH of the sodium silicate solution was adjusted to 10 by addition of a cation exchange resin. Four milliliters of the active silica solution was added to the APTS/gold nanoparticle suspension under vigorous stirring. Further polymerization of active silica in the solution (at pH \sim 8.5) was allowed to proceed for one day. The resulting silica shells on the gold nanoparticles were imaged by transmission electron microscopy, and had an average thickness of 2 nm.

Sample Preparation. To disperse the nanoparticles for experiments, a 3 μL sample of gold nanoparticle solution was placed on a coverslip that had been treated with (3-acryloxypropyl)trimethoxysilane to improve adhesion of the final polymeric structures.⁴⁷ The sample was then placed in an oven at 110 $^\circ\text{C}$ for 3 min to evaporate the solvent.

The acrylic resin used was composed of 54 wt % dipentaerythritol pentaacrylate esters (Sartomer), 43 wt % tris(2-hydroxyethyl) isocyanurate triacrylate (Sartomer), and 3 wt % Lucirin TPO-L (BASF). After thorough mixing, one drop of the resin was placed on the nanoparticle-coated substrate. A layer of Scotch tape was placed on the coverslip as a spacer, and then a second coverslip was placed on top of the tape. The sandwiched sample was mounted on a computer-controlled, 3D, piezoelectric nanostage (Physik Instrumente).

Imaging and Fabrication. A tunable Ti:sapphire laser (Coherent Mira 900-F) produced pulses of 150 fs duration at a repetition rate of 76 MHz. The beam was introduced into an inverted microscope (Zeiss Axiovert 100) through the reflected light-source port and was directed to the objective by a dichroic mirror. A 1.45 NA, 100 \times , oil-immersion objective (Zeiss α Plan-FLUAR) was used for MAIL imaging and multiphoton fabrication. Scanning was performed with the piezoelectric sample stage or with a set of galvanometric mirrors. The luminescence signal was collected by a single-photon-counting avalanche photodiode (EG&G) and the signal was transferred to a computer with use of a data acquisition board (National Instruments). Data collection and image construction were performed with software written in LabView (National Instruments).

For MAIL imaging, typically an area of 30 μm^2 was scanned with 140 \times 140 pixel resolution in \sim 10 s. Filters that cut off the excitation light were placed before the detector. MEMAP was performed under similar conditions or simultaneously with MAIL imaging. MAP was used to create markers on the substrate so that the same sample region could be located reproducibly. For SEM imaging, samples were sputter-coated with approximately 10 nm of Pt/Pd. Shown in Figure 1 are a typical gold MAIL spectrum²⁶ along with the one-photon

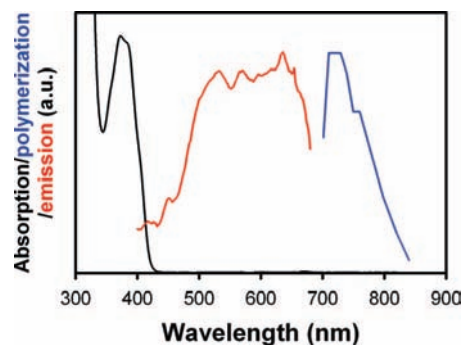


Figure 1. One-photon absorption spectrum (black) and two-photon polymerization action spectrum (blue) of Lucirin TPO-L and a typical MAIL emission spectrum for gold nanoparticles (red).

absorption and two-photon polymerization action spectra of Lucirin TPO-L.⁴⁷

III. Results

Our initial experiments focused on correlating MAIL efficiency with nanoparticle morphology. Gold nanoparticles were coated on a glass coverslip and MAIL experiments were performed with 800 nm excitation. The excitation intensity was less than 2 mW at the sample. Typical MAIL data are shown as 3D and contour plots in panels a and b of Figure 2, respectively. The luminescent regions span a broad range of intensities, as has been observed previously.²⁶

A scanning electron micrograph of the same region of the gold nanoparticle sample is shown in Figure 2c. It is apparent from this image that there are significant aggregates of nanoparticles on the substrate. In general, the regions of brightest luminescence correspond with the positions of aggregates. To explore this correspondence in more detail, in Figure 3 we show an overlay of the matching regions of the MAIL image and the electron micrograph. The aggregate of three nanoparticles marked A has only modest MAIL intensity, whereas the larger aggregates B and C both exhibit considerably brighter luminescence. The luminescence intensity does not appear to be linear in the number of particles in an aggregate, however, but rather depends upon the aggregate structure as well. This enhancement of emission due to aggregation is reminiscent of the effects that have been seen in SERS, in which aggregates can have considerably larger field enhancements than do single nanoparticles.^{11,24}

To investigate the origin of MAIL further, we studied particles with a 2 nm coating of silica. As we observed previously,²⁶ the silica coating does not lead to any significant change in MAIL behavior. SEM studies of samples of silica-coated particles indicated the presence of aggregates similar to those observed for uncoated nanoparticles. As also was the case for the uncoated nanoparticles, we found a strong correlation between aggregation and luminescence intensity in the coated particles. The aggregate shape again plays an important role in determining the luminescence intensity of the silica-coated nanoparticles.

We also examined the effect that the 10-nm coating of Pt/Pd that was applied to the samples for SEM imaging had on MAIL. Pt/Pd films on glass do not exhibit MAIL, and gold nanoparticles that are encapsulated completely in Pt/Pd would not be expected to luminesce. However, the majority of particles that luminesced before coating the substrate with Pt/Pd also luminesced afterward, albeit with a somewhat diminished intensity. Thus, coating particles and aggregates on one side with another metal does not have a substantial influence on MAIL efficiency. There was

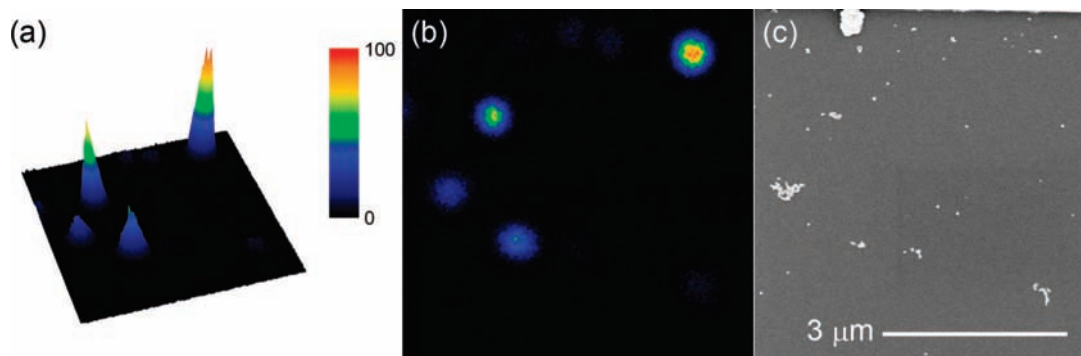


Figure 2. (a) 3D and (b) contour plots of MAIL from gold nanoparticles deposited on a glass substrate and excited with 800 nm light. The intensity scale is the same for both images. (c) A scanning electron micrograph of the same region of the sample.

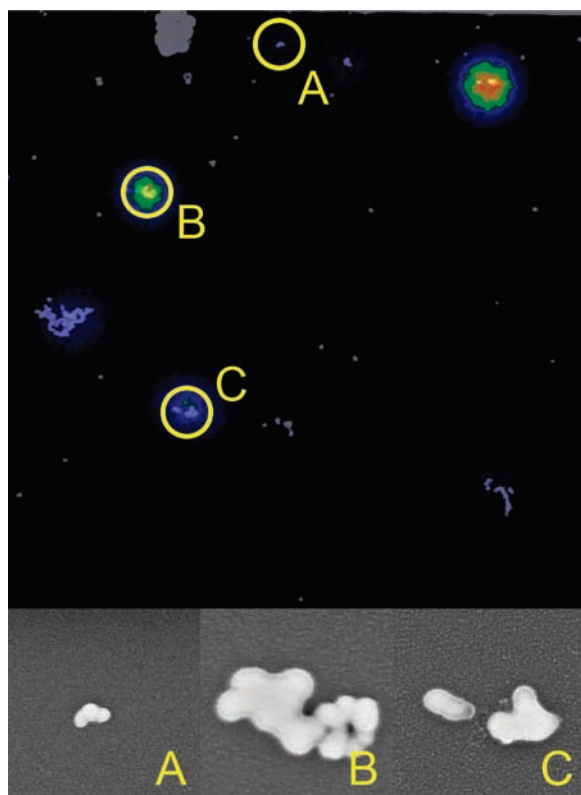


Figure 3. An overlay of the MAIL and SEM images from Figure 2 (top) and close-up electron micrographs of selected emitting aggregates (bottom). The magnifications of the close-ups vary.

no obvious correlation of particle shape or aggregation with the areas in which the MAIL did disappear upon Pt/Pd coating.

Our previous studies have demonstrated that MAIL from gold nanoparticles involves a three-photon excitation process at 800 nm.²⁶ Similar results were obtained for 900 nm excitation.²⁶ This observation is surprising, since other studies have shown MAIL from different gold structures to arise from two-photon excitation at 800 nm.^{27,31,33,34} Furthermore, neither 800 nor 400 nm light is within the plasmon band of the gold nanoparticles employed here, so plasmonic enhancements would not be expected to be significant. We believe that the implication of these results is that our experimental protocol selects for particles or aggregates of particles that have a particularly large three-photon-absorption cross-section.²⁹ It is additionally possible that the aggregates that exhibit strong MAIL with 800 nm light have collective plasmon bands that are red-shifted enough to have significant absorption at this wavelength.

If the efficiency of MAIL depends upon shifted plasmon bands in aggregates, then the MAIL efficiency of different

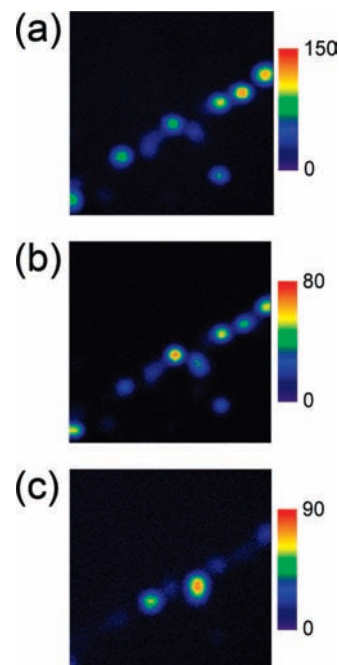


Figure 4. Contour plots of MAIL from gold nanoparticles on the same region of a glass substrate excited with (a) 725, (b) 800, and (c) 890 nm light.

aggregates would be expected to be a function of excitation wavelength. To explore this issue, we performed MAIL experiments on the same region of a sample with 725, 800, and 890 nm excitation. Representative MAIL images from one such study are shown in Figure 4. For 725 and 800 nm light, the excitation power was less than 2 mW at the sample, whereas for 890 nm light the excitation power was on the order of 10 mW at the sample. The images for 725 and 800 nm excitation are similar. With 890 nm excitation, the most prominent MAIL emission arises from regions that do not luminesce as strongly with shorter wavelength excitation. Comparison with an SEM image of the same region did not reveal a clear correlation between structure and the wavelength dependence of the MAIL efficiency, but our results suggest that at least for long-wavelength excitation aggregates with significantly red-shifted plasmon bands may be involved.

We next turn to MEMAP and its correlation with MAIL. The radical photoinitiator used for these studies, Lucirin TPO-L, has a two-photon polymerization action spectrum that has a peak at 725 nm (Figure 1). The polymerization action spectrum is negligibly small at wavelengths longer than 850 nm.⁴⁷ We first performed experiments at 800 nm, a wavelength at which MAP can easily be performed with this photoinitiator.⁴⁷ Prepolymer

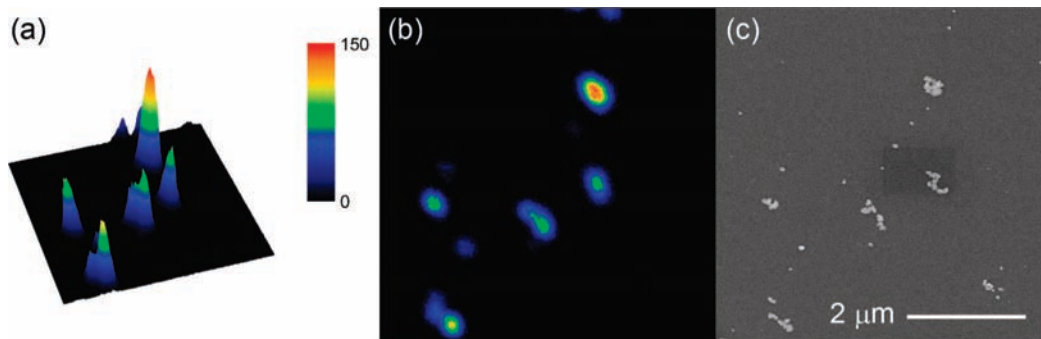


Figure 5. (a) 3D and (b) contour plots of MAIL from gold nanoparticles deposited on a glass substrate, immersed in prepolymer resin, and excited with 800 nm light. The intensity scale is the same for both images. (c) A scanning electron micrograph of the same region of the sample.

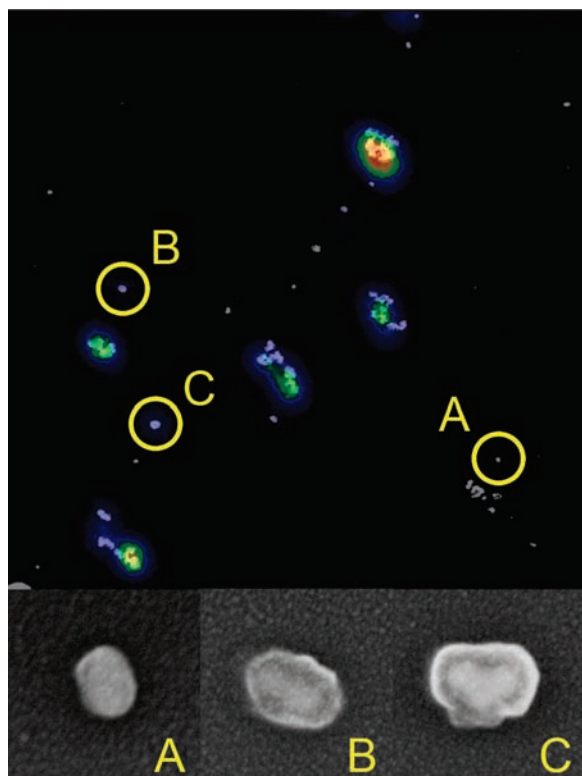


Figure 6. An overlay of the MAIL and SEM images from Figure 5 (top) and close-up electron micrographs of selected particles and aggregates without a polymer shell (bottom left) and with a polymer shell (bottom center and bottom right). The magnifications of the close-ups vary.

resin was placed on top of a substrate that had been coated with gold nanoparticles. The laser beam was scanned over the sample at an intensity too low to lead to polymerization in the pure prepolymer resin but high enough to obtain high-quality MAIL images. A MAIL image from a representative sample is shown in 3D form in Figure 5a and as a contour plot in Figure 5b.

An SEM image of the same sample area (Figure 5c) demonstrates the presence of both individual nanoparticles and aggregates. Overlapping the MAIL and SEM images reveals that once again the brightest emission arises from regions that contain aggregates of particles (Figure 6). Nanoparticles that do not show strong MAIL emission, such as particle A in Figure 6, do not exhibit any polymerization. However, particles or aggregates that do exhibit MAIL such as B and C in Figure 6, also have a polymer coating. Similar results were obtained with excitation at 725 nm.

If the prepolymer resin is prepared without any photoinitiator, MAIL emission is observed but polymerization does not occur

even at high laser intensity. We can therefore conclude the photoinitiator is essential for MEMAP. This result implies that multiphoton excitation does not lead to ejection of electrons from the gold nanoparticles, at least in quantities sufficient to cause polymerization.

Our results indicate that there is a direct correspondence between MAIL and MEMAP. This conclusion is consistent with the results of previous studies in indicating that field enhancement can lead to being able to perform MAP at lower intensities than is possible in the absence of noble-metal structures.^{34,39–41} However, we must still establish the role played by field enhancement in MEMAP. One possibility is that field enhancement increases the effective two-photon absorption cross section of nearby photoinitiator molecules. This mechanism has been assumed to be the source of MEMAP in previous reports.^{34,39–41} However, MAIL from gold occurs across the visible spectrum,²⁶ and so it is also possible that the emitted light causes polymerization directly by exciting the photoinitiator molecules. Indeed, it is due to this second potential mechanism that we call the effect metal-enhanced MAP rather than field-enhanced MAP.

Our observations offer a number of clues into the mechanism of MEMAP in gold nanoparticles and aggregates. First, field enhancement is expected to occur in localized hot spots in nanoparticle aggregates. Because polymerization takes place in a solvent-free resin in our system, radicals do not diffuse over a significant distance before reacting. Thus, field-enhanced two-photon absorption would be expected to lead to asymmetric polymerized regions around aggregates with hot spots. However, the polymerized region is generally spread uniformly about the aggregates for which MEMAP occurs. Second, the pattern of field enhancement is expected to be dependent upon the polarization of the light. We have observed no preference for the polymerized pattern to be stretched or otherwise affected along the polarization axis of the excitation light. Third, silica coating of the nanoparticles does not have any appreciable effect on the efficiency of MEMAP. Taken together, these factors suggest that MEMAP in this system does not arise from field-enhanced two-photon absorption of the photoinitiator.

To seek more definitive evidence for the origin of MEMAP, we performed experiments using 890 nm excitation. Because the two-photon absorption cross section of Lucirin TPO-L is vanishingly small at this wavelength, in the absence of gold nanoparticles we were not able to observe MAP in the prepolymer resin even at very high laser powers (~ 100 mW) of 890 nm light.

Shown in panels a and b of Figure 7 are 3D and contour plots, respectively, of MAIL from gold particles in the prepolymer resin excited by 890 nm light with approximately 6 mW

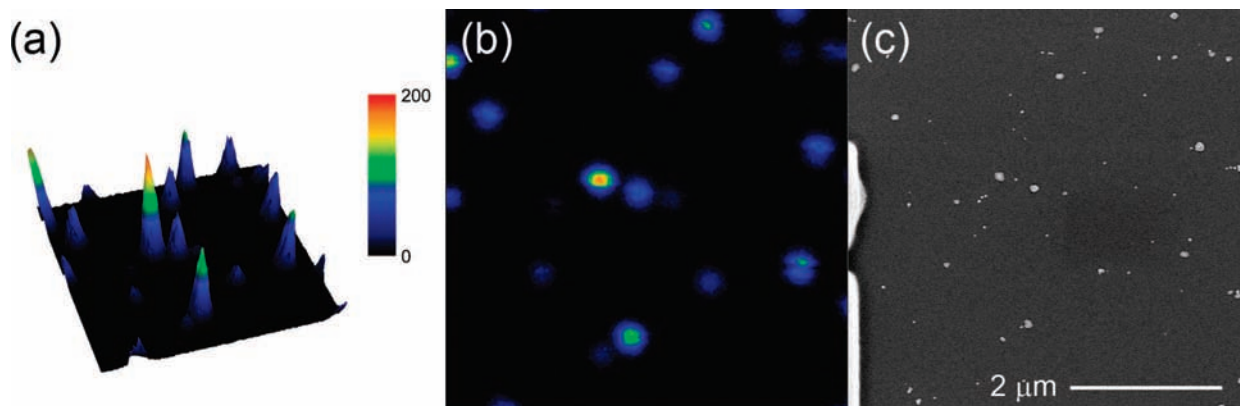


Figure 7. (a) 3D and (b) contour plots of MAIL from gold nanoparticles deposited on a glass substrate, immersed in prepolymer resin, and excited with 890 nm light. The intensity scale is the same for both images. (c) A scanning electron micrograph of the same region of the sample.

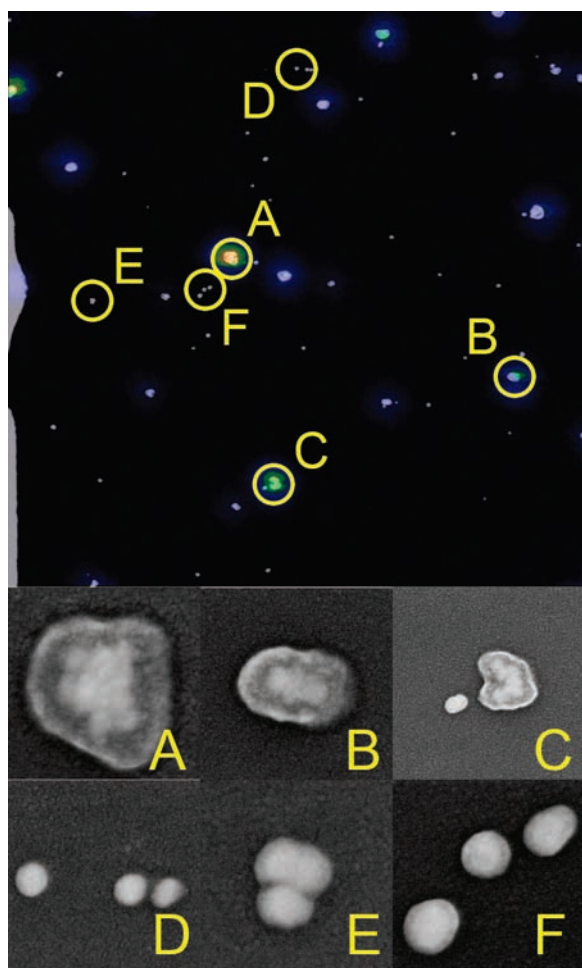


Figure 8. An overlay of the MAIL and SEM images from Figure 7 (top) and close-up electron micrographs of selected particles and aggregates with a polymer shell (middle) and without a polymer shell (bottom). The magnifications of the close-ups vary.

of excitation power at the sample. The corresponding SEM image of this region of the sample is shown in Figure 7c. The overlap of the MAIL and SEM images (Figure 8) shows once again that larger aggregates tend to have higher emission intensities.

Also shown in Figure 8 are close-up SEM images of different particles and aggregates. Aggregates A, B, and C all show strong MAIL emission and have polymerized shells around them. However, the particles and aggregates D, E, and F do not exhibit detectable MAIL emission at this excitation intensity and do

not have polymerized shells about them. Once again there is a direct correspondence between MAIL emission and MEMAP.

IV. Discussion

The results presented here clarify a number of issues regarding field-enhanced phenomena of gold nanoparticles. While our studies have focused on MAIL and MEMAP, what we have learned may have implications for other processes that depend on field enhancement as well.

Our first important observation is that efficient MAIL generally arises from aggregates rather than from single particles. This result is consistent with previous observations that aggregates of nanoparticles give considerably stronger SERS enhancements than do single particles.^{11,23} Not all aggregates of the same size lead to MAIL emission, indicating that shape plays an important role in this process as well. For instance, we rarely observe strong MAIL signals from linear aggregates, even when they contain four or more particles. Additionally, the emission efficiency for different aggregates depends upon the excitation wavelength. Thus, high MAIL efficiency may in part result from having a plasmon band that is sufficiently red-shifted to overlap well with the excitation wavelength. However, our results suggest that the plasmon band is not the only important factor in MAIL.

The second important observation is that there is a strong correspondence between the particles and aggregates that exhibit strong MAIL and those that exhibit strong MEMAP. We can conclude from this result that MAIL and MEMAP both depend on field enhancement. However, as discussed above a number of facets of our results with 800 nm excitation call into question whether MEMAP occurs through field enhancement of the two-photon absorption of the photoinitiator molecules.

The third key observation is that MEMAP occurs with 890 nm laser pulses, even though two-photon excitation of the photoinitiator is not possible at this wavelength. The most likely explanation for this phenomenon is that three-photon excitation of the nanoparticles leads to MAIL emission that in turn excites the photoinitiator. Thus, in our system MEMAP is likely to be a consequence of MAIL rather than a direct effect of field enhancement. It remains possible that field enhancement promotes *three*-photon excitation of the photoinitiator, but we view this explanation as unlikely for a number of reasons. First, even at very high excitation powers (on the order of 100 mW) it is not possible to excite the photoinitiator directly with three 890 nm photons. Second, as discussed above, the MEMAP process creates a polymer shell that extends over the entire nanoparticle or aggregate, and does not show any elongation

along the direction of the laser polarization. A field-enhancement hot spot may drive emission anywhere within an aggregate, but is likely to have a considerably more localized effect on polymerization. MAIL emission is expected to be relatively isotropic, and so would lead to uniform polymer shells around luminescent regions of nanostructures. The bandwidth of our laser pulses is small enough (~ 10 nm) that we can also rule out two-photon excitation of the photoinitiator from photons at the blue tail of the laser spectrum when the center wavelength of the pulses is 890 nm.

As the results of our MEMAP experiments are similar for excitation wavelengths ranging from 725 to 890 nm, it appears likely that the mechanism is the same over this entire tuning range. It remains possible that enhanced two-photon absorption and excitation via MAIL emission both play a role in MEMAP at the shorter wavelengths, but as the qualitative features of MEMAP are independent of wavelength over the range studied, we believe that the latter mechanism dominates in all of our experiments.

It is natural to ask whether the mechanism that is responsible for MEMAP in our system was also operative in previous reports of this effect.^{34,39–41} It is not possible to give a definitive answer for this question at present, as different nanostructures, photoinitiators, and polymer systems were used in the previous studies. MAIL emission was observed in gold nanobowties, and was strongest in the region in which MEMAP occurred.³⁴ However, MAIL in the bowtie system arose from two-photon absorption, and so the essential physics may be different from that of our nanoparticles and aggregates. It will be interesting to employ wavelength-dependent studies to investigate the mechanism for MEMAP in these other systems.

Finally, we should also consider whether MAIL plays a role in other field-enhanced effects of noble-metal nanostructures. For instance, SERS is known to be most efficient in dimers or other aggregates of nanoparticles.^{11,23} However, calculations of the field enhancements available from such aggregates cannot account for the highest observed enhancements of Raman scattering. In a full quantum treatment of spontaneous Raman scattering, a vacuum field at the scattered frequency is involved.⁴⁸ Any process that increases the field at the scattered frequency above the vacuum level will act to increase the efficiency of the SERS process, and so it is possible that MAIL plays a role in this technique under some circumstances.

The studies reported here were performed with ultrafast lasers, and SERS is generally performed with CW lasers. MAIL with CW lasers would be expected to be a weak effect, but we should note that MEMAP has been reported with an incoherent light source.⁴⁰ Even a weak MAIL effect may have the potential to increase the efficiency of SERS measurably.

V. Conclusions

In this paper we have explored the connection between two field-enhanced phenomena of noble-metal nanostructures, MAIL and MEMAP. Aggregation of nanoparticles increases the efficiency of both of these phenomena. We have found a strong correlation between particles and aggregates that exhibit MAIL and MEMAP. On the basis of wavelength-dependent studies, we believe that the predominant mechanism for MEMAP in the systems studied here is MAIL-mediated excitation of the photoinitiator rather than field-enhanced two-photon absorption. This mechanism may be relevant for other field-enhanced phenomena of noble metal nanoparticles as well.

Acknowledgment. We appreciate the support of the Maryland NanoCenter and its NispLab. The NispLab is supported

in part by the NSF as a MRSEC Shared Experimental Facility. This work was supported in part by the UMD-NSF-MRSEC under grant DMR 05-20471.

References and Notes

- (1) Kelly, K. L.; Coronado, E.; Zhao, L. L.; Schatz, G. C. *J. Phys. Chem. B* **2003**, *107*, 668.
- (2) Schwartzberg, A. M.; Zhang, J. Z. *J. Phys. Chem. C* **2008**, *112*, 10323.
- (3) Yang, W. H.; Schatz, G. C.; Vanduyne, R. P. *J. Chem. Phys.* **1995**, *103*, 869.
- (4) Bell, S. E. J.; Sirimuthu, N. M. S. *Chem. Soc. Rev.* **2008**, *37*, 1012.
- (5) Tian, Z. Q.; Ren, B.; Wu, D. Y. *J. Phys. Chem. B* **2002**, *106*, 9463.
- (6) Kneipp, K.; Wang, Y.; Kneipp, H.; Perelman, L. T.; Itzkan, I.; Dasari, R.; Feld, M. S. *Phys. Rev. Lett.* **1997**, *78*, 1667.
- (7) Nie, S.; Chiu, D. T.; Zare, R. N. *Science* **1994**, *266*, 1018.
- (8) Qian, X. M.; Nie, S. M. *Chem. Soc. Rev.* **2008**, *37*, 912.
- (9) Pieczonka, N. P. W.; Aroca, R. F. *Chem. Soc. Rev.* **2008**, *37*, 946.
- (10) Kneipp, J.; Kneipp, H.; Kneipp, K. *Chem. Soc. Rev.* **2008**, *37*, 1052.
- (11) Camden, J. P.; Dieringer, J. A.; Wang, Y. M.; Masiello, D. J.; Marks, L. D.; Schatz, G. C.; Van Duyne, R. P. *J. Am. Chem. Soc.* **2008**, *130*, 12616.
- (12) Lal, S.; Grady, N. K.; Kundu, J.; Levin, C. S.; Lassiter, J. B.; Halas, N. J. *Chem. Soc. Rev.* **2008**, *37*, 898.
- (13) Goutev, N.; Futamata, M. *Appl. Spectrosc.* **2003**, *57*, 506.
- (14) Osawa, M. Surface-enhanced infrared absorption. In *Near-Field Optics and Surface Plasmon Polaritons*; Springer: New York, 2001; Vol. 81, p 163.
- (15) Cai, W. B.; Amano, T.; Osawa, M. *J. Electroanal. Chem.* **2001**, *500*, 147.
- (16) Osawa, M.; Ataka, K.; Yoshii, K.; Nishikawa, Y. *Appl. Spectrosc.* **1993**, *47*, 1497.
- (17) Kawata, S.; Verma, P. *Chimia* **2006**, *60*, A770.
- (18) Kawata, S.; Ichimura, T.; Hayazawa, N.; Inouye, Y.; Hashimoto, M. *J. Nonlinear Opt. Phys. Mater.* **2004**, *13*, 593.
- (19) Ichimura, T.; Hayazawa, N.; Hashimoto, M.; Inouye, Y.; Kawata, S. *Phys. Rev. Lett.* **2004**, *92*.
- (20) Hayazawa, N.; Ichimura, T.; Hashimoto, M.; Inouye, Y.; Kawata, S. *J. Appl. Phys.* **2004**, *95*, 2676.
- (21) Xu, H. X.; Aizpurua, J.; Kall, M.; Apell, P. *Phys. Rev. E* **2000**, *62*, 4318.
- (22) GarciaVidal, F. J.; Pendry, J. B. *Phys. Rev. Lett.* **1996**, *77*, 1163.
- (23) Michaels, A. M.; Jiang, J.; Brus, L. *J. Phys. Chem. B* **2000**, *104*, 11965.
- (24) Michaels, A. M.; Nirmal, M.; Brus, L. E. *J. Am. Chem. Soc.* **1999**, *121*, 9932.
- (25) Boyd, G. T.; Yu, Z. H.; Shen, Y. R. *Phys. Rev. B* **1986**, *33*, 7923.
- (26) Farrer, R. A.; Butterfield, F. L.; Chen, V. W.; Fourkas, J. T. *Nano Lett.* **2005**, *5*, 1139.
- (27) Beversluis, M. R.; Bouhelier, A.; Novotny, L. *Phys. Rev. B* **2003**, *68*, 115433.
- (28) Eichelbaum, M.; Schmidt, B. E.; Ibrahim, H.; Rademann, K. *Nanotechnology* **2007**, *18*.
- (29) Kempa, T.; Farrer, R. A.; Giersig, M.; Fourkas, J. T. *Plasmonics* **2006**, *1*, 45.
- (30) Durr, N. J.; Larson, T.; Smith, D. K.; Korgel, B. A.; Sokolov, K.; Ben-Yakar, A. *Nano Lett.* **2007**, *7*, 941.
- (31) Kim, H. M.; Xiang, C. X.; Guell, A. G.; Penner, R. M.; Potma, E. O. *J. Phys. Chem. C* **2008**, *112*, 12721.
- (32) Gong, H. M.; Zhou, Z. K.; Xiao, S.; Su, X. R.; Wang, Q. Q. *Plasmonics* **2008**, *3*, 59.
- (33) Su, X. R.; Li, M.; Zhou, Z. K.; Zhai, Y. Y.; Fu, Q.; Huang, C.; Song, H.; Hao, Z. H. *J. Lumin.* **2008**, *128*, 642.
- (34) Sundaramurthy, A.; Schuck, P. J.; Conley, N. R.; Fromm, D. P.; Kino, G. S.; Moerner, W. E. *Nano Lett.* **2006**, *6*, 355.
- (35) Eichelbaum, M.; Kneipp, J.; Schmidt, B. E.; Panne, U.; Rademann, K. *ChemPhysChem* **2008**, *9*, 2163.
- (36) LaFratta, C. N.; Fourkas, J. T.; Baldacchini, T.; Farrer, R. A. *Angew. Chem., Int. Ed.* **2007**, *46*, 6238.
- (37) Maruo, S.; Fourkas, J. T. *Laser Photon. Rev.* **2008**, *2*, 100.
- (38) Rumi, M.; Barlow, S.; Wang, J.; Perry, J. W.; Marder, S. R. Two-Photon Absorbing Materials and Two-Photon-Induced Chemistry. In *Photoreactive Polymers I*; Springer: Berlin, 2008; Vol. 213; pp 1.
- (39) Postnikova, B. J.; Currie, J.; Doyle, T.; Hanes, R. E.; Anshyn, E. V.; Shear, J. B.; Vanden Bout, D. E. *Microelectron. Eng.* **2003**, *69*, 459.
- (40) Ueno, K.; Juodkazis, S.; Shibuya, T.; Yokota, Y.; Mizeikis, V.; Sasaki, K.; Misawa, H. *J. Am. Chem. Soc.* **2008**, *130*, 6928.
- (41) Yin, X.; Fang, N.; Zhang, X.; Martini, I. B.; Schwartz, B. J. Near-Field Multiphoton Nanolithography Using an Apertureless Optical Probe. In *Nonlinear Optical Transmission and Multiphoton Processes in Organics*;

Yeates, A. T.; Belfield, K. D.; Kajzar, F.; Lawson, C. M., Eds.; SPIE: Bellingham, WA, 2003; p 96.

(42) Jang, S. M.; Park, J. S.; Shin, S. M.; Yoon, C. J.; Choi, B. K.; Gong, M. S.; Joo, S. W. *Langmuir* **2004**, *20*, 1922.

(43) Enustun, B. V.; Turkevich, J. *J. Am. Chem. Soc.* **1963**, *85*, 3317.

(44) Turkevich, J.; Stevenson, P. C.; Hillier, J. *Discuss. Faraday Soc.* **1951**, 55.

(45) Garcia-Santamaria, F.; Salgueirino-Maceira, V.; Lopez, C.; Liz-Marzan, L. M. *Langmuir* **2002**, *18*, 4519.

(46) Liz-Marzan, L. M.; Giersig, M.; Mulvaney, P. *Langmuir* **1996**, *12*, 4329.

(47) Baldacchini, T.; LaFratta, C.; Farrer, R. A.; Teich, M. C.; Saleh, B. E. A.; Naughton, M. J.; Fourkas, J. T. *J. Appl. Phys.* **2004**, *95*, 6072.

(48) Loudon, R. *The Quantum Theory of Light*, 2nd ed; Oxford University Press: New York, 1983.

JP811072R